

Allylimidazolium salt based antibacterial polymer coatings produced by thiol–ene photocuring



Mirinae Kim^{a,e}, Chiman Song^b, Dong Keun Han^c, Kwang-Duk Ahn^{c,*}, Seung Sang Hwang^d, Dong June Ahn^{e,*}, Man-Ho Kim^{a,*}

^a Advanced Analysis Center, Korea Institute of Science and Technology, 136-791 Seoul, Republic of Korea

^b Chemical Kinomics Research Center, Korea Institute of Science and Technology, 136-791 Seoul, Republic of Korea

^c Center for Biomaterials, Korea Institute of Science and Technology, 136-791 Seoul, Republic of Korea

^d Center for Materials Architecturing, Korea Institute of Science and Technology, 136-791 Seoul, Republic of Korea

^e Department of Chemical & Biological Engineering and KU-KIST Graduate School of Converging Science & Technology, Korea University, 136-701 Seoul, Republic of Korea

ARTICLE INFO

Article history:

Received 19 August 2014

Received in revised form 30 December 2014

Accepted 4 January 2015

Available online 13 January 2015

Keywords:

Antibacterial coating
Antibacterial polymers
Allylimidazolium salts
Thiol–ene photocuring
Mass fractal network

ABSTRACT

Photocurable formulations containing trifunctional thiol, trifunctional ene, and antibacterial allylimidazolium salts have been employed for transparent antibacterial coatings. The antibacterial component 1-allyl-3-dodecylimidazolium salt (ADIm) is prepared and chemically attached to polymer networks using a one-step thiol–ene photocuring reaction. Ultra-small (USANS) and small angle neutron scattering (SANS) measurements show that the photocured polymers are loosely networked three-dimensional structures with a mass fractal of approximately 2.7 ± 0.2 . The minimum inhibitory concentration (MIC) for the ADIm was determined to be 500 $\mu\text{g/ml}$ and 15.63 $\mu\text{g/ml}$ for *Escherichia coli* (Gram negative) and *Staphylococcus aureus* (Gram positive) bacteria, respectively. Coating formulations containing 10 mol% of the antibacterial ADIm photocured on glass substrates showed strong antibacterial activity against environmental bacteria such as *E. coli* and/or *S. aureus*.

© 2015 Elsevier B.V. All rights reserved.

1. Introduction

The public has increasingly become concerned about hygiene in everyday life. People share many objects with others such as door knobs, handles on public transportation vehicles, and touch screens, as well as personal objects such as cell phones, all of which can be contaminated by bacteria that cause communicable diseases [1]. It has been estimated that approximately 3–5% of patients leave the hospital with a nosocomial infection [2]. Bacteria-laden surfaces of intravenous poles and furniture in healthcare facilities can be sources for the pathogenic bacteria to spread to the public. Manufacturing objects with antibacterial materials could be a good alternative to reduce the probability of such infections. For example, metallic materials such as silver and copper have antimicrobial activity [3,4], which either inhibit bacterial growth or kill bacteria attached to surfaces. However, the replacement of touchable objects currently in use with antibacterial materials is not cost effective. Conventional antibacterial agents also have limitations when applied to solid surfaces. For release-type antibacterial mate-

rials, the physically-mixed antibacterial ingredient is in a matrix, (e.g., dispersing antimicrobial in paint) and gradually leaks out over time. Antibacterial function is reduced by leaching and exhaustion of the low molecular weight antibacterial chemicals. Therefore, it is desirable to design new antibacterial materials and methods that do not leach and can be applied specifically to target surfaces while maintaining their original structural properties. To prevent antimicrobial agents from leaching, chemical binding of antibacterial monomers to polymer chains has been performed [5–16]. An effect of chain length on antibacterial activity was observed in homopolymers of quaternary ammonium salts (QASs) with different alkyl lengths [11], hydrophobic polycationic coatings [13], ionic liquids [14], and functionalized polyether ether ketone surfaces [15]. Most of these antibacterial materials require complicated design and application procedures. A simple method to fix the antibacterial ingredients to a cotton fabric using ultraviolet photocuring has been shown to kill waterborne pathogenic bacteria [17]. An overview of antibacterial mechanisms and new trends in antibacterial polymers has been reviewed [6–10,16,18]. Studies have focused on various antibacterial polymers [6,9,10], possible applications of zwitterionic materials to kill bacteria [7], antibacterial material surfaces with polyelectrolyte multilayers

* Corresponding authors.

E-mail addresses: kdahn@kist.re.kr (K.-D. Ahn), ahn@korea.ac.kr (D.J. Ahn), man-hokim@kist.re.kr (M.-H. Kim).

[8], biopassive and bioactive coatings [16], and the conformation of polymers or peptides [18]. Antibacterial polymers can maintain their antibacterial function even when cleaned so they can be applied to clothes, bedding, and medical fabric products [19,20].

Our strategies to design such antibacterial materials are the following: First, the materials must have strong antibacterial activity. Second, the antibacterial activity must be sustained on the applied surface for a long time. Third, the materials must be easily applied, coated, and fixed on the surface of existing end-user products for hospitals, public facilities, household and private items, apparel products, packing materials, food containers, and so on. Fourth, the antibacterial materials must allow the products to be used as quickly as possible. Fifth, the material preparation process must be environmentally friendly and the antibacterial materials must be eco-friendly, not contaminating the environment by leaching toxic chemicals.

To achieve these results, we have permanently attached antibacterial imidazolium (Im) salt-based chemicals to a cross-linked polymer backbone by using thiol–ene photocuring. There are number of reports about antibacterial polymers containing ammonium or IM as an antibacterial QASs by post-reactions or grafting to enhance the antibacterial effect [12,21–25]. A vinyl imidazolium was covalently grafted to castor oil [21], and incorporated into the backbone chain in an alternating manner with a hydrophobic aryl group [22], or as a side group in polysiloxane [12]. Antibacterial quaternary ammonium salts were photocrosslinked in the form of polymeric ionic hydrogel films with a cross-linker of poly(ethylene oxide) dimethacrylate [23], or a coating film with diacrylic resins [24]. In addition, Thymole-doped acrylic resins also show antibacterial activity by releasing thymol in liquid media [25]. Among practically useful photocuring processes, thiol–ene photocuring is known to have a few significant advantages, such as high photo-sensitivity and thermal stability, insensitivity of the oxygen inhibition effect, and ready handling of low odor chemical ingredients [26,27]. Various multifunctional ‘thiol’ and ‘ene’ components are commercially available and applied in ‘thiol–ene’ photocuring systems with a proper combination of photoinitiators (PI). As for antibacterial agents, some QASs with long alkyl chains are known to have high antimicrobial activity and are widely used as disinfectants in hospitals (complying with the 1st condition). Many Im salts are mostly stable ionic liquids as well as useful green solvents [28–30]. We have designed antibacterial Im QASs with both long alkyl and allyl groups as a photoreactive QAS component to incorporate into polymer chains, thereby preventing the leaching of chemicals and sustaining the antibacterial activity for longer periods (complying with the previously mentioned 2nd condition). The photocurable liquid formulations have adequate viscosity to allow easy and uniform spreading of the antibacterial coating on the target surface (complying with the 3rd condition). The photocurable thiol–ene formulations allow rapid curing reactions, (complying with the 4th condition) and the photocuring process is simple and environmentally-friendly as no toxic organic solvents are used (complying with the 5th condition).

Antibacterial activity was tested on two bacterial strains, Gram negative (*Escherichia coli*) and Gram positive (*Staphylococcus aureus*), with different cell wall properties, which can be models for other similar bacteria.

2. Experimental

2.1. Materials and instruments

1-Allylimidazole and 1-bromododecane were purchased from Across Organics (NJ, USA). Trimethylolpropane tris(3-mercaptopropionate) (TMPTSH), 2,4,6-triallyloxy-1,3,5-triazine (TAOTA), and other chemicals were purchased from Sigma–Aldrich Chem. and

used without further purification. For comparison, a commercial disinfectant benzalkonium chloride (BKC) was purchased from Sigma–Aldrich Chem. A photoinitiator, 1-hydroxycyclohexyl phenyl ketone (HCPK, Irgacure184), was provided from Ciba Specialty Chemicals, Swiss.

¹H NMR spectra were recorded on a Varian Gemini 200 spectrometer using deuteriochloroform (CDCl₃) as an internal standard. FT-IR Spectra of before and after UV irradiation were recorded on a Nicolet-360 spectrophotometer (USA) from 400 to 4000 cm⁻¹ at a resolution of 4 cm⁻¹ with a liquid sample on a NaCl plate and with a photocured film of approximately 30 μm thickness, respectively. The Mass Spectrum of ADIm was measured on a Q-TOF Synapt G2 High Definition Mass Spectrometer (Waters, Manchester, UK) under the following conditions: sampling cone voltage 40 V, capillary voltage 3 kV, source temperature 120 °C, desolvation temperature 400 °C, cone N₂ gas flow 100 L/hr, and devolution N₂ gas flow 800 L/hr. ADIm was dissolved in DMSO, then diluted with 400 μL MeOH. Data were obtained from 50 to 800 Da. The tendency of the photocuring reaction was measured under a nitrogen atmosphere using a Differential Photocalorimeter (DPC 930, TA Instrument, USA) with a 200 W Hg-lamp (light intensity, 10 mW/cm²) attached. Samples of approximately 5–8 mg were placed in open aluminum pans. Thermogravimetric analysis (TGA) of the photocured films was conducted with a TA instruments TGA 2950 (USA) at a heating rate of 10 °C/min under a nitrogen atmosphere.

Ultra small angle scattering neutron scattering (USANS) and small angle scattering neutron scattering (SANS) were measured with the KIST-USANS and HANARO 18 m-SANS, covering micro to nanometer size scales in the range of scattering vectors $2 \times 10^{-5} \text{ \AA}^{-1} < Q (= (4\pi \sin \theta) / \lambda) < \sim 2 \times 10^{-2} \text{ \AA}^{-1}$, where 2θ is the scattering angle and λ is the neutron wavelength, $\lambda = 4 \text{ \AA}$ for USANS and $\lambda = 4.45 \text{ \AA}$ and 8.28 \AA for SANS. The scattering intensities were converted to the absolute scale ($d\Sigma(Q)/d\Omega$) by correcting the instrument parameters, transmission, and sample thickness.

2.2. Synthesis of 1-allyl-3-dodecylimidazolium bromide (ADIm)

The desired antibacterial component, 1-allyl-3-dodecylimidazolium bromide, was prepared by a reaction of *N*-allylimidazole (5.00 g, 46.2 mmol) with dodecylimidazolium bromide (11.49 g, 46.2 mmol) in DMF at 60 °C for 12 h. The reaction mixture solution was added to an Erlenmeyer flask with a large excess of diethyl ether, stirred for approximately 30 min, and allowed to stand until the organic layer separated. When layers formed, the top layer of diethyl ether was removed. This procedure was repeated approximately 3–4 times. Once the diethyl ether was removed, a small amount of ethyl alcohol was added and then was evaporated at 65 °C and 130–140 rpm. The ADIm was further dried in a vacuum oven until the weight became constant and the yield was approximately 60%. ¹H NMR (CDCl₃, 400 MHz): 10.58 (a, 1H), 7.38 (b, 2H), 7.38 (b, 2H), 6.03 (d, 1H), 5.48 (c, 2H), 5.08 (e, 2H), 4.34 (f1, 2H), 1.92 (f2, 2H), 1.24–1.40 (f3–f11, 18H), 0.87 (f12, 3H). (Refer to Fig. 1 for identification of peaks.) Additionally, the mass spectrum shows a mass value identical to the theoretical mass, $m/z = 277$, for ADIm, C₁₈H₃₃N₂Br. The small fraction of $m/z = 278$ and 279 is due to the natural isotopes.

2.3. Photocuring process and characterization

All the formulations containing ADIm, TMPTSH and TAOTA were prepared in total 100 mol% with a fixed photoinitiator (PI) composition of HCPK (5 mol%) in additional quantity. For example, to make 10 mol% of ADIm content in the photocured polymers, ADIm 0.073 g, TMPTSH 0.357 g, TATO A 0.225 g, and HCPK 0.001 g were used. For practical photocuring, the liquid samples were coated mainly on a slide. The photocuring procedure in the literature

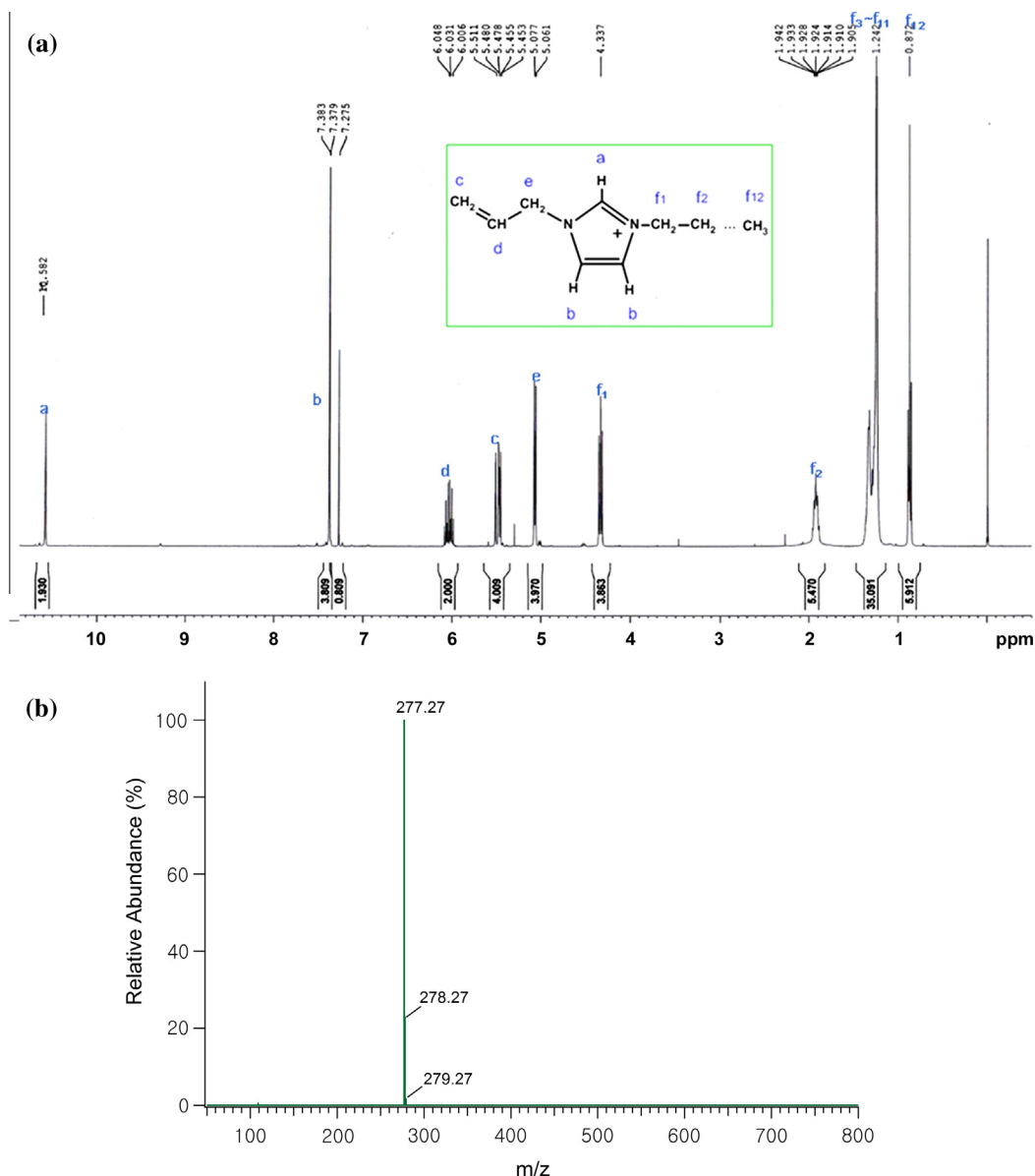


Fig. 1. NMR spectrum (a) and MS spectrum (b) of the antibacterial ADIm, allyl-3-dodecylimidazolium salt.

was used [31]. The liquid photocuring formulations were coated (20 mm × 40 mm width, 20–35 μm thickness) on a slide glass with an applicator (Mitutoyo, Japan), then UV curing was performed with a exposure time of 5 s/run (5 m/min conveyor belt speed, 200 mJ/cm²) using conveyor-type UV-curing equipment (Exposure Model LZ-UH101, Lichtzen Co., Ltd., Korea). Photocuring tendency was evaluated by rubbing the photocured coatings with methyl ethyl ketone (MEK) solvent. The gel content was determined from weight loss of the film dried after refluxing MEK in Soxlet at 80 °C for 24 h.

2.4. Evaluation of antibacterial activity

2.4.1. Bacterial strains and antibacterial susceptibility testing of ADIm

The MIC (minimum inhibitory concentration) of the ADIm component was determined by the agar dilution method using 14 bacterial strains (*S. aureus* ATCC 65389, *S. aureus* ATCC 25923, *Enterobacter cloacae* ATCC 27508, *E. coli* ATCC 10536, *E.*

coli ATCC 25922, *Bacillus subtilis* ATCC 6633, *Bacillus cereus* ATCC 27348, *Salmonella typhimurium* ATCC 13311, *S. typhimurium* ATCC 14028, *Acinetobacter calcoaceticus* ATCC 15473, *Micrococcus luteus* ATCC 9341, *Moraxella catanhalis* ATCC 25240, *Serratia marcescens* ATCC 27117 and *Proteus vulgaris* ATCC 6059) (ATCC, American Type Culture Collection, VA, USA). All of the strains were maintained on nutrient agar (Difco Laboratories, MI, USA) at 37 °C. ADIm was incorporated into Mueller–Hinton agar (MHA, Difco Laboratories, MI, USA) at various final concentrations (1000, 500, 250, 125, 62.5, 31.25, 15.63 and 7.81 μg/ml). Bacterial inoculums were prepared from overnight cultures in nutrient broth at 37 °C. The MHA plates containing ADIm were inoculated with the prepared inoculums using a multipoint inoculator (MIC-2000, Dynatech Laboratories Inc., USA) and incubated for 24 h at 37 °C. The MIC of the ADIm was defined as the lowest concentration that visibly inhibited the growth of each bacterium and was compared with that of a commercial disinfectant, BKC.

2.4.2. Antibacterial activity testing of polymer coatings

Antibacterial activities of polymer-coated glasses were determined using a slightly modified parallel streak method (AATCC TM147). Two bacterial strains, Gram positive *S. aureus* ATCC 65389 and Gram negative *E. coli* ATCC 10536, were used for the antibacterial activity test. The former was chosen because of its high infection rate in humans and the latter because of it had the lowest MIC value among Gram negative bacteria (see Appendix A, Supplementary Table 2).

Cover slips coated with different types of imidazolium compounds by photocuring were autoclaved at 121 °C for 15 min and thoroughly dried. Inoculums of the two bacterial strains were prepared by incubation in nutrient broth for 24 h at 37 °C. The bacterial inoculums were streaked on MHA plates and cover slips coated with different photocured samples were also placed on the plates, and the plates were incubated for 24 h at 37 °C. The antibacterial activity of the polymer-coated glass was detected qualitatively by observing the clear area of inhibited bacterial growth beneath and along the sides of the cover slip.

3. Results and discussion

3.1. Preparation and antibacterial activity of ADIm

Im salt as an “ene” component, the 1-allyl-3-dodecylimidazolium bromide (ADIm) salt, was prepared by reacting *N*-allylimidazole with dodecylimidazolium bromide in DMF solvent [see Appendix A, Supplementary Figure 8]. The structure of ADIm was confirmed with NMR and Q-TOF MS. The NMR peak of 4.34 (f1, 2H) related to a new bond N—CH₂— between the dodecyl group and imidazolium group indicated the successful synthesis of the antibacterial ADIm component as shown in Fig. 1. The mass value in the MS is identical with the theoretical mass $m/z = 277$ of ADIm. Both NMR and Q-TOF MS confirmed the synthesized product as ADIm.

3.2. Evaluation of antibacterial activity of ADIm

The antibacterial activity of the ADIm component against Gram positive and Gram negative bacteria was evaluated. The minimum inhibitory concentration (MIC) for the ADIm monomer was determined for 14 bacterial strains at 17 different ADIm/(water + Agar + nutrient broth) concentrations ranging from 1000 µg/ml to 0.015 µg/ml. The results of the MIC test including photos are shown in Fig. 2. Representative Gram positive and Gram negative bacteria were selected based on the MIC values for the antibacterial activity test of the photocured polymer coatings. The MIC values of the ADIm against *S. aureus* (ATCC 65389) and *E. coli* (ATCC 10536) were 500 µg/ml and 15.63 µg/ml, respectively, which were found to be comparable to that of a commercial disinfectant, BKC. The MIC values for the 14 bacterial strains are listed in Appendix A, Supplementary Table 2.

3.3. Photocured antibacterial polymers and characterization

To provide the antibacterial coatings without leaching, highly sensitive photocurable formulations have been developed based on the thiol–ene photocuring. As shown in Scheme 1, the antibacterial ADIm was formulated with trifunctional thiol TMPTSH and trifunctional ene TAOTA with HCPK as a PI.

The photocurable liquid formulation was applied onto the surface of a slide glass plate with a thickness of approximately 25 µm and then UV irradiated to initiate the thiol–ene reaction of the coating. The thiol–ene reaction produced solidified transparent films in which the antibacterial ADIm was directly incorporated into the polymer network as shown in Scheme 2.

The photocuring reaction of the formulation was monitored by the exotherm peak of the differential photocalorimetry (DPC) (Fig. 3). The exotherm peaks almost disappeared within 60 s, indicating that most reactions were finished within 1 min. With increasing ADIm content, the exotherm peaks decreased and shifted to longer reaction times (Fig. 3-(a)); thus, ADIm may inhibit the thiol–ene photoreactions. In the absence of ADIm, the exotherm peak indicates typical high photo-reactivity of the thiol–ene photocuring. Similar phenomena were also observed with the PI content in the formulations as shown in Fig. 3-(b). With decreasing PI content, the exotherm peaks decreased and shifted to longer reaction times. The IR spectra of the thiol–ene photocuring reaction was checked (Fig. 4). The characteristic absorption bands of the thiol groups at 2570 cm⁻¹ and carbon–carbon double bonds at 937 and 1648 cm⁻¹ disappeared and a new carbon–sulfur band was observed at 680 cm⁻¹. Weak residual peaks of —SH and C=C group indicate the existence of a small amount of un-reacted groups.

Upon photocuring, the photocured coatings produced transparent flexible freestanding films by fast photocuring as confirmed by DPC and FT-IR spectral analysis. To confirm that the ADIm and other chemical components were chemically-networked by the photocuring, the gel content and antibacterial activity were measured. These data are summarized in Table 1. A control sample, a formulation containing TMPTSH (50 mol%) and TAOTA (50 mol%) without ADIm, showed nearly complete photocuring with a gel content of 99%. With an increasing ADIm content from 1 mol% to 20 mol%, the gel content decreased from 99% to 90%, indicating that some low molecular components, such as oligomers, were extracted. Achieving a gel content of 100% via the photocuring process is still challenging. The formulation with 10 mol% ADIm showed a high gel content of 95% and antibacterial activity towards both Gram positive and Gram negative bacteria; thus, this formulation could be a candidate for an antibacterial photocuring coating.

The photocured films containing 5, 10, and 20 mol% of the active ADIm salt permitted no bacterial growth of the representative bacterial *S. aureus* and *E. coli* strains. It is evident that the antimicrobial ADIm was combined with a thiol component to form a networked polymer structure or at least was chemically bonded to the backbone chains, which show strong antibacterial activity against environmental bacteria in everyday life. Thus, the antibacterial components might not leach out of the polymer coating as they are chemically bound together.

The structure of the film was investigated with USANS and SANS measurements for the cured antibacterial film with an ADIm content of 10 mol%. Fig. 5 shows the measured USANS and SANS intensities and the fractal model fit using the NCNR SANS analysis macro [32,33]. The correlation length (ξ) and mass fractal (D_m) were estimated from the following structure factor $S(Q, r_o, \xi, D_m)$ that represents the spatial order [32–34]

$$\frac{d\Sigma(Q)}{d\Omega} \sim cS(Q, r_o, \xi, D_m) + KQ^{-p} + bkg \quad (1)$$

$$S(Q, r_o, \xi, D_m) = 1 + \frac{D_m \Gamma(D_m - 1) \sin[(D_m - 1) \arctan(Q\xi)]}{(Qr_o)^{D_m}} \times \left(1 + \frac{1}{Q^2 \xi^2}\right)^{\frac{1-D_m}{2}} \quad (2)$$

where, c is a scale factor including the contrast and volume fraction, p is the scattering power index, K is a constant, $\Gamma(D_m - 1)$ is the gamma function of $(D_m - 1)$, and r_o is the radius of the individual scatterers (i.e., building blocks). When the value of D_m (i.e., slope in the plot of $d\Sigma(Q)/d\Omega$ vs Q) is in the range of $2 < D_m < 3$ in the scattering profile, it indicates that the materials consist of a mass fractal.

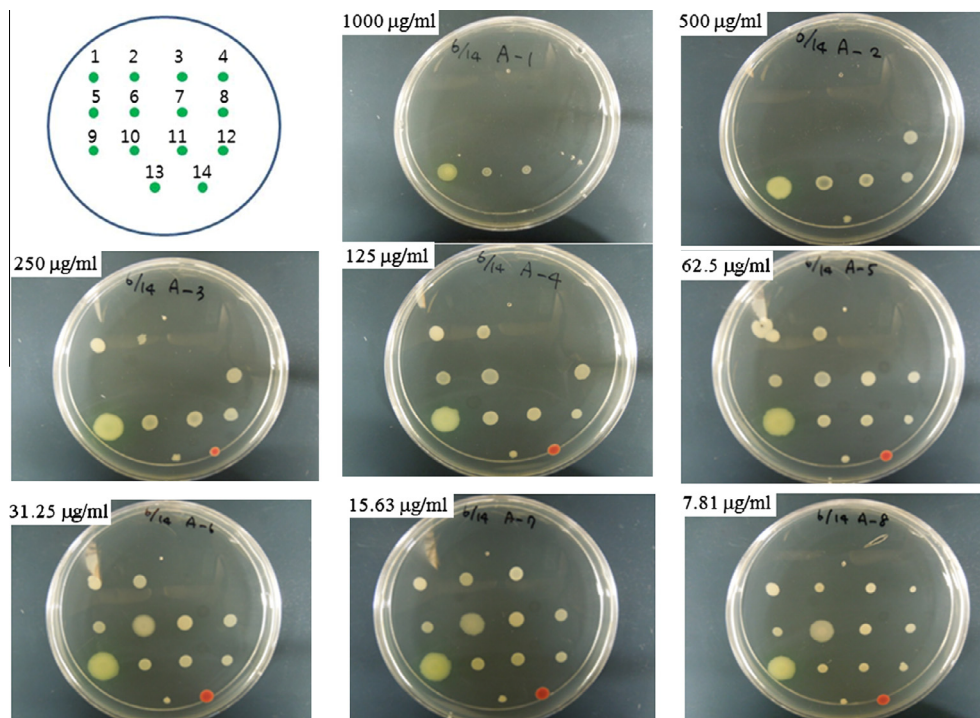
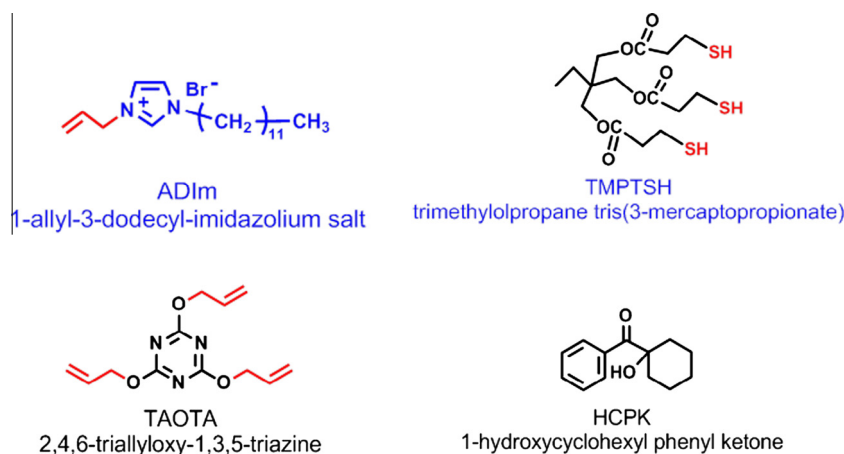


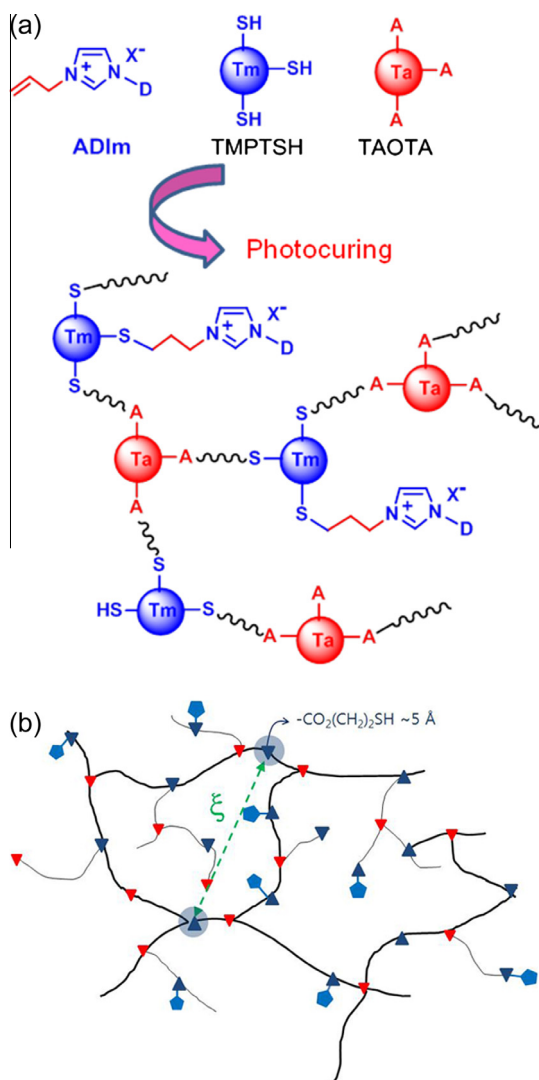
Fig. 2. MIC test of ADIm for 14 different species of Gram positive and Gram negative bacteria; 1: *Staphylococcus aureus* ATCC 65389, 2: *Staphylococcus aureus* ATCC 25923, 3: *Enterobacter cloacae* ATCC 27508, 4: *Escherichia coli* ATCC 10536, 5: *Escherichia coli* ATCC 25922, 6: *Bacillus subtilis* ATCC 6633, 7: *Bacillus cereus* ATCC 27348, 8: *Salmonella typhimurium* ATCC 1331, 9: *Salmonella typhimurium* ATCC 14028, 10: *Acinetobacter calcoaceticus* ATCC 15473, 11: *Micrococcus luteus* ATCC 9341, 12: *Moraxella catanhalis* ATCC 25240, 13: *Serratia marcescens* ATCC 27117, 14: *Proteus vulgaris* ATCC 6059.



Scheme 1. Photocurable formulations consisting of multifunctional 'thiol' and 'ene' for antibacterial polymer coatings.

The functional group ($-\text{CO}_2(\text{CH}_2)_2\text{SH}$) with a radius of 5.2 \AA in TMPTSH was selected as a junction site, which approximately matches with the cold neutron wavelength of USANS and SANS. Other functional groups with a radius of $1\text{--}10 \text{ \AA}$ could have been chosen, but the change in D_m and ξ values was less than 1%. Fitting was performed by fixing the parameter of $r_o \sim 5.0 \text{ \AA}$ in the Q range of $8.9 \times 10^{-5} \text{ \AA}^{-1} < Q < 0.087 \text{ \AA}^{-1}$ with a constant background while the other parameters, ξ , D_m , and c were floating. K and $p \sim -2.9$ in the low Q upturn ($Q < 5 \times 10^{-5} \text{ \AA}^{-1}$) were pre-esti-

mated from independent fitting and then summed two scattering fittings to cover the entire scattering Q ranges. The curvature around $\sim 10^{-5} \text{ \AA}^{-3}$ may be due to the form factor oscillation attributed to the density fluctuation distribution from a heterogeneous domain in the network. Despite the curvature, the overall slope in the range $3 \times 10^{-2} \text{ \AA}^{-1} < Q < 5 \times 10^{-2} \text{ \AA}^{-1}$ is approximately $D_m = -2.7 \pm 0.2$, which indicates that the thiol-ene photocured antibacterial polymer containing ADIm salt consists of a mass fractal-like network (i.e., a somewhat open network structure). The



Scheme 2. Schematic representation of photocured thiol-ene networked polymers (a) and correlation length between junctions (b). Triangular shapes of blue and red represent TMPTSH and TAOTA, respectively. Light blue pentagon symbols indicate the antibacterial ADIm components. Thick lines represent the crosslinked chains while thin lines represent dangling chains. The functional group, $(-\text{CO}_2(\text{CH}_2)_2\text{SH})$, of TMPTSH is assumed as a junction site of scattering. (For interpretation of the references to colour in this figure legend, the reader is referred to the web version of this article.)

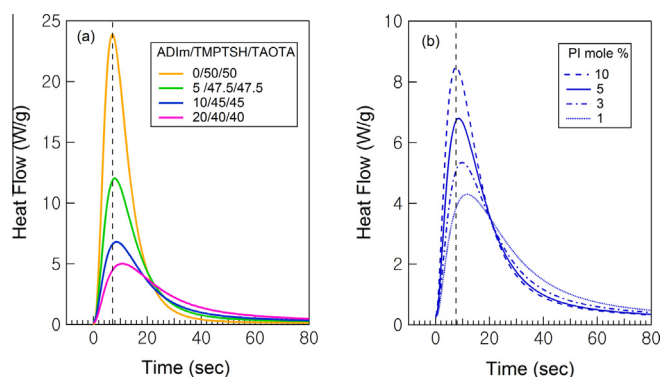


Fig. 3. DSC measurements of various photocurable antibacterial formulations; (a) with different ingredient ratios (indicated) at a fixed concentration of photoinitiator (5 mol%) and (b) with various PI contents (mol%) at a fixed ADIm content (10 mol%).

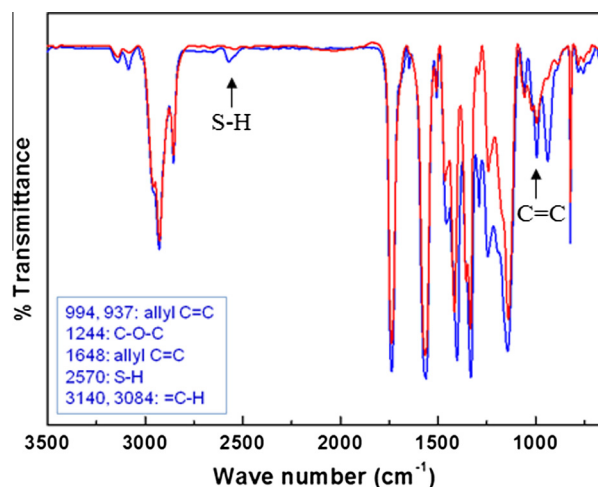


Fig. 4. Comparison of FT-IR spectra before (blue) and after (red) photocuring with ADIm (20 mol%), ADIm/TMPTSH/TAOTA (20/40/40 mol ratio), showing the disappearance of thiol groups by thiol-ene reactions. (For interpretation of the references to colour in this figure legend, the reader is referred to the web version of this article.)

average correlation distance between the junctions of the cross-linked polymers is approximately $\xi \sim 535 \pm 10$ nm. Such a large ξ can indicate the photocured antibacterial polymers are loosely networked including branched chains as schematically shown in Fig. 3(b), which agrees with the mass fractal network. The bulky ADIm could be a reason for the mass fractal-like loose network. The residual allyl double bonds in FTIR, a decrease in the exotherm of DPC, and the high gel content also indicate a loose network structure of the photocured film containing an ADIm functional group.

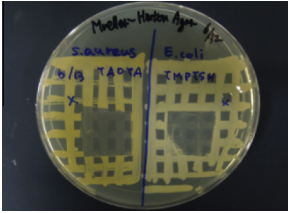
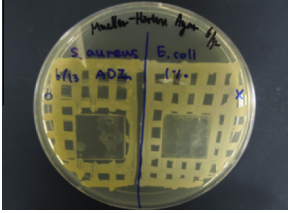
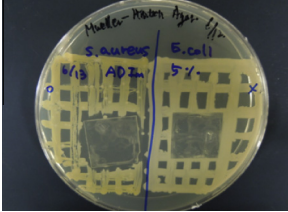
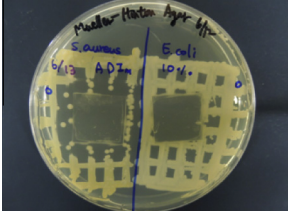
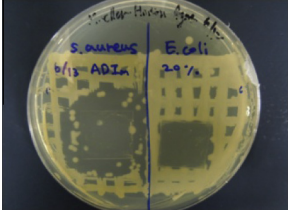
The thermal stability of the photocured ADIm-containing polymer film is stable up to approximately 200 °C as shown by the TGA measurement (Fig. 6), indicating that the sterilizing temperature of 121 °C of the polymer film chosen for the antibacterial activity test does not degrade the polymer coating. Thermal decomposition gradually occurs from 200 °C to approximately 350 °C followed by the rapid decomposition at ~ 400 °C.

3.4. Antibacterial activity test of photocured polymer coatings

Antibacterial activity of the photocured polymer films is shown in Table 1. The polymer coated surface of the glass plates was placed in contact with the cultivated *S. aureus* and *E. coli*, including three controls, the bacterial streak itself [see Appendix A, Supplementary Figure 7], the glass plate with no coating placed on the streak, and the glass plate coated with the photocured coating with TMPTSH and TAOTA in the absence of ADIm. Bacterial streaks were unaffected in the three controls, indicating that the treatments had no antibacterial activity for *S. aureus* or *E. coli*. The bacterial streaks of both *S. aureus* and *E. coli* did not grow in the presence of the photocured films at a concentration of 10 and 20 mol% of ADIm in the polymer chains. At 5 mol% of ADIm, antibacterial activity against *E. coli* was not observed. The original streak grew under the coated glass. However, antibacterial activity against *S. aureus* occurred at a concentration as low as 1 mol% of ADIm. The results indicate that the ADIm-attached photocured polymer films kill the bacteria and/or prohibit bacterial growth.

This observation indicates that the ADIm components play a role as an antibacterial functional moiety present on a surface so that direct contact with bacteria is possible.

Table 1
Antibacterial activity with ADIm content including two controls, empty glass, and TMPTSH:TAOTA [50:50], and gel content of the corresponding photocured films.

Composition (mol%) [ADIm/TMPTSH/TAOTA] ^a	Antibacterial activity ^b				Gel contents ^c (wt%)
	<i>S. aureus</i> [ATCC 65389]	<i>E. coli</i> [ATCC 10536]	<i>S. aureus</i> [ATCC 65389]	<i>E. coli</i> [ATCC 10536]	
Control with cover glass			X	X	
Control ADIm 0%			X	X	99
ADIm 1%			O	X	97
ADIm 5%			O	X	96
ADIm 10%			O	O	95
ADIm 20%			O	O	90

^a Mole ratio of TMPTS and TAOTA are equal depending on ADIm content. (e.g. ADIm 10% indicates ADIm/TMPTSH/TAOTA [10:45:45]).

^b Symbol ○ represents no bacterial growth and symbol x represents bacterial growth. Yellow streaks are bacteria (see [Appendix A, Supplementary Figure 7](#)).

^c Gel content was measured after extraction in refluxing MEK.

4. Conclusion

We have prepared an antibacterial 1-allyl-3-dodecylimidazolium salt (ADIm) monomer and used it in antibacterial polymer coatings created with easily processable thiol-ene photocuring. The liquid coating formulations consisting of ADIm, a commercial trifunctional thiol and ene compounds underwent thin film formation via a one-stop photocuring reaction, which allowed the antibacterial

Im salt to chemically bind to the crosslinked polymer backbone. The photocured film showed a loosely networked mass fractal-like structure. On solid surfaces, the photocured film demonstrated strong antibacterial activity against *E. coli* and/or *S. aureus* that depended solely on the ADIm concentration (5–10 mol%) in the polymer coatings. These antibacterial coatings prevent leaching of antibacterial agents and toxic chemicals to the environment. Taking advantage of conventional thiol-ene photocuring, the antibacterial

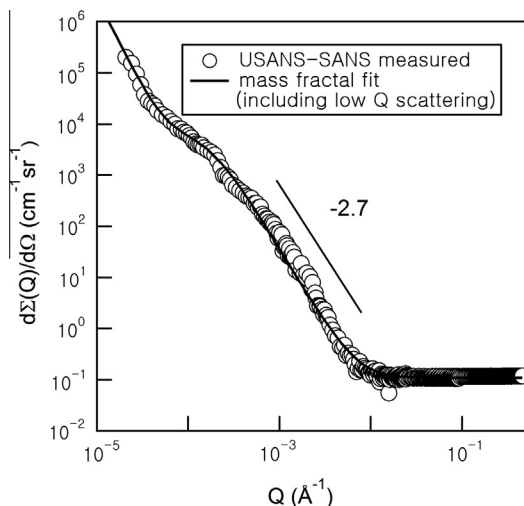


Fig. 5. USANS-SANS curve of photocured antibacterial polymer containing 10% ADIm. The solid line is a model-fit with a mass fractal including a very low Q scattering of approximately 10^{-5} \AA^{-1} .

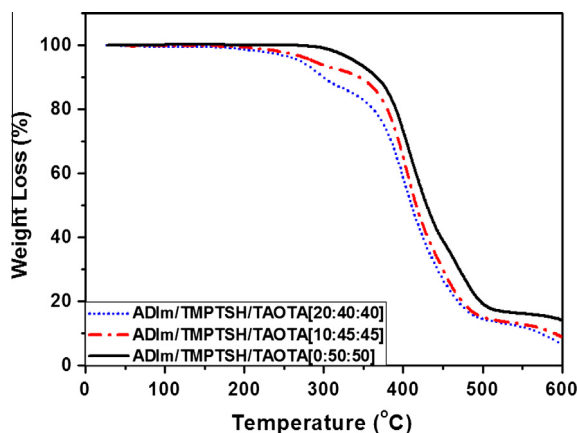


Fig. 6. TGA measurement of photocured antibacterial films as a function of ADIm content and a fixed PI concentration (5 mol%).

coating process is simple and practical and thus could be applied to various objects to improve hygiene while not leaching out the antibacterial chemicals.

Acknowledgements

MHK acknowledges partial financial support from Korea Institute of Science and Technology (2v03611). DJA acknowledges the support by the National Research Foundation (MSIP 2014023305, 2014010072) of Korea. We have benefited from Dr. Seong, B.K. of the HANARO at Korea Atomic Energy Research Institute for experimental support of 18 m-SANS. A part of this work was presented

at the 13th RadTech Asia held during May 20 to 24, 2013 in Shanghai, China. Reviewers provided valuable comments.

Appendix A. Supplementary material

Supplementary data associated with this article can be found, in the online version, at <http://dx.doi.org/10.1016/j.reactfunctpolym.2015.01.001>.

References

- [1] R.R.W. Brady, P. Kalima, N.N. Damani, R.G. Wilson, M.G. Dunlop, *Ann. R. Surg. Eng.* 89 (2007) 656–660.
- [2] D.R. Schaberg, D.H. Culver, R.P. Gaynes, *The Am. J. Med.* 91 (suppl. 3B) (1991) 3B-72S–3B-75S.
- [3] A. Mikolay, S. Huggett, L. Tikana, G. Grass, J. Braun, D.H. Nies, *Appl. Microbiol. Biotech.* 87 (2010) 1875–1879.
- [4] J.C. Tiller, C.-J. Liao, K. Lewis, A.M. Klibanov, *PNAS* 98 (11) (2001) 5981–5985.
- [5] G. Lu, D. Wu, R. Fu, *Reac. Func. Polym.* 67 (2007) 355–366.
- [6] A. Muñoz-Bonilla, M. Fernandez-Garcia, *Prog. Polym. Sci.* 37 (2012) 281–339.
- [7] S. Jiang, Z. Cao, *Adv. Mater.* 22 (2010) 920–932.
- [8] J.A. Lichter, K.J. Van Viet, M.F. Rubner, *Macromolecules* 42 (2009) 8573–8586.
- [9] El-Refaie Kenawy, S.D. Worley, R. Broughton, *Biomacromolecules* 8 (2007) 1359–1384.
- [10] T. Tashiro, *Macromol. Mater. Eng.* 286 (2001) 63–87.
- [11] C.Z. Chen, N.C. Beck-Tan, P. Hurjati, T.K. van Dyk, R.A. LaRossa, S.L. Cooper, *Biomacromolecules* 1 (2000) 473–480.
- [12] U. Mizerska, W. Fortuniak, J. Chojnowski, R. Halasa, A. Konopacka, W. Werel, *Eur. Polym. J.* 45 (2009) 779–787.
- [13] T.P. Schaer, S. Stewart, B.B. Hsu, A.M. Klibanov, *Biomaterials* 33 (2012) 1245–1254.
- [14] M.B. Yagci, S. Bolca, J.P.A. Heuts, W. Ming, G. de With, *Prog. Org. Coat.* 72 (2011) 343–347.
- [15] A. Yousaf, A. Farrukh, Z. Oluz, E. Tuncel, H. Duran, S.Y. Dogan, T. Tekinay, H. Rehman, B. Yameen, *Reac. Func. Polym.* 83 (2014) 70–75.
- [16] M. Charnley, M. Textor, C. Acikgoz, *Reac. Func. Polym.* 71 (2011) 329–334.
- [17] B.B. Hsu, A.M. Klibanov, *Biomacromolecules* 12 (2011) 6–9.
- [18] A.C. Engler, N. Wiradharma, Z.Y. Ong, D.J. Coady, J.L. Hedrick, Y.-Y. Yang, *Nano Today* 7 (2012) 201–222.
- [19] K.-D. Ahn, J.-H. Kang, Korea Patent KR 10-0752150, South Korea, 2007.
- [20] K.-D. Ahn, J.-H. Kang, D.K. Han, Korea Patent KR 01-0748041, South Korea, 2007.
- [21] G. Totaro, L. Cruciani, M. Vannini, G. Mazzola, D. Di Gioia, A. Celli, L. Sisti, *Eur. Polym. J.* 56 (2014) 174–184.
- [22] L. Liu, Y. Huang, S.N. Riduan, S. Gao, Y. Yanga, W. Fanb, Y. Zhanga, *Biomaterials* 33 (2012) 8625–8631.
- [23] H. He, B. Adzima, M. Zhong, S. Averick, R. Koepsel, H. Murata, A. Russell, D. Luebke, A. Takahara, H. Nulwala, K. Matyjaszewski, *Multifunctional Photocrosslinked Polymeric Ionic Hydrogel Films*, The Royal Society of Chemistry, 2014.
- [24] G. Gozzelino, C. Lisanti, S. Beneventi, *Eng. Aspects* 430 (2013) 21–28.
- [25] M.D. Esposti, F. Pilati, M. Bondi, Simona de Niederhäusern, R. Iseppi, M. Toselli, *J. Coat. Technol. Res.* 10 (2012) 371–379.
- [26] C.E. Hoyle, T.Y. Lee, T. Roper, *J. Poly. Sci. Part A: Polym. Chem.* 42 (2004) 5301–5338.
- [27] M.J. Kade, D.J. Burke, C.J. Hawker, *J. Poly. Sci. Part A: Polym. Chem.* 48 (2010) 743–750.
- [28] M.J. Earle, K.R. Seddon, *Pure Appl. Chem.* 72 (2000) 1391–1398.
- [29] J.G. Huddleston, A.E. Visser, W.M. Reichert, H.D. Willauer, G.A. Broker, R.D. Rogers, *Green Chemistry* 3 (2001) 156–164.
- [30] A. Romero, A. Santos, J. Tojo, A. Rodríguez, *Journal of Hazardous Materials* 151 (2008) 268–273.
- [31] K.-D. Ahn, M.-H. Kim, *Prog. Org. Coat.* 73 (2012) 194–201.
- [32] S.R. Kline, *J. Appl. Cryst.* 39 (2006) 895–900.
- [33] J. Teixeira, *J. Appl. Cryst.* 21 (1988) 781–785.
- [34] L.M. Anovitz, G.W. Lynn, D.R. Cole, G. Rother, L.F. Allard, W.A. Hamilton, L. Porcar, M.-H. Kim, *Geochimica et Cosmochimica Acta* 73 (2009) 7303–7324.